Theoretical model for the Mpemba effect through the canonical first-order phase transition

Sheng Zhang and Ji-Xuan Hou*
School of Physics, Southeast University, Nanjing 211189, China

(Received 15 May 2022; accepted 9 September 2022; published 23 September 2022)

The Mpemba effect is the phenomenon in which the system with high initial temperature cools faster than the system with low initial temperature when all other conditions are the same. A theoretical model of the Mpemba effect through the canonical first-order phase transition is proposed in this paper, which shows that in the cooling processes, the path of the first-order phase transition of the system with the high initial temperature does not pass through any metastable state, while the path of the first-order phase transition of the system with the low initial temperature passes through a metastable state, which leads to the occurrence of the Mpemba effect. Then an example of the theoretical model is given in the Blume-Emery-Griffiths model. The Monte Carlo algorithm is adopted to calculate the estimated times for both systems with different initial temperature to cool down and undergo a first-order phase transition. The simulation results demonstrate a Mpemba effect in the system. Moreover, the evolution paths of the first-order phase transitions of the systems with high and low initial temperatures are given, respectively. The theoretical model presented here may help explain the Mpemba effect in water.

DOI: 10.1103/PhysRevE.106.034131

I. INTRODUCTION

If two glasses of water with the same macroscopic properties except for the initial temperature are placed in the same environment to cool down, the water with the higher initial temperature might freeze faster. Aristotle, Francis Bacon, and Descartes all described this counterintuitive phenomenon in different ways [1,2], but it was not until it was rediscovered by a high school student that it was named after him—the Mpemba effect [3]. The Mpemba effect is when two systems, with the same macroscopic physical quantities except for the initial temperature, are placed in the same cooling environment, and the system with the higher initial temperature will enter the cryogenic phase faster. Up to now, there has been no consensus on the specific mechanism of the Mpemba effect, and various explanations about this effect have been given, such as the microscopic structure of intramolecular hydrogen-oxygen covalent bonds and intermolecular hydrogen bonds [4,5], convection [6,7], hydrodynamic effects [7], gas dissolved in water [8,9], evaporation [10,11], and so on [12,13]. Moreover, the Mpemba-like effect was presented recently. The Mpemba-like effect is when two samples of a substance whose macroscopic parameters are all the same (except for the initial temperatures) are both in thermal contact with the same low-temperature heat source at the same time, and the hotter one will take less time to reach the low temperature. The Mpemba effect or the Mpemba-like effect is also widely reported in systems other than water, such as nanotube resonators [14], granular fluid [15] or gases [16,17], magnetoresistance alloys [18], spin glasses [19], clathrate hydrates [20], polymers [21], and so on [22–24].

Several theories have now been developed to explain the mechanism of the Mpemba-like effect in certain systems. Lasanta *et al.* proposed that the Mpemba-like effect of granular fluid is due to the fact that the rate of change of temperature with time is not only related to temperature, but also to its parameter a_2, which relates to the speed distribution of the granular particles [15]. Baity-Jesi *et al.* pointed out that the Mpemba-like effect of spin glasses is due to the fact that the cooling process depends on both the temperature and the coherence length of the system [19]. Lu and Raz explained the Mpemba-like effect of a three-state system, the Ising model, and diffusion dynamics by introducing nonequilibrium path and relaxation mode analysis, which led to a general condition for the Mpemba effect to occur in any Markov dynamical system [25]. However, the above are all theoretical explanations for the Mpemba-like effect without any phase transitions. There are also studies on the Mpemba effect with phase transitions. Yang and Hou proposed the non-Markovian Mpemba effect in the microcanonical ensemble of a mean-field system [26,27]. Luo and Sommer proposed a possible mechanism for the Mpemba effect of the first-order phase transition in polymer crystallization [28]. Very recently, Holtzman and Raz used the phenomenological Landau phase transition theory to determine the second-order phase transition time, and they gave a model with the Mpemba effect of a second-order phase transition in the canonical ensemble [29].

In this paper, we present a theoretical model of the Mpemba effect through the canonical first-order phase transition. The model shows that the cooling path of the first-order phase transition of the system with the high initial temperature does not pass through any metastable state, while the cooling path of the first-order phase transition of the system with the low initial temperature passes through a metastable state, which leads to the occurrence of the Mpemba effect. The

*jxhou@seu.edu.cn

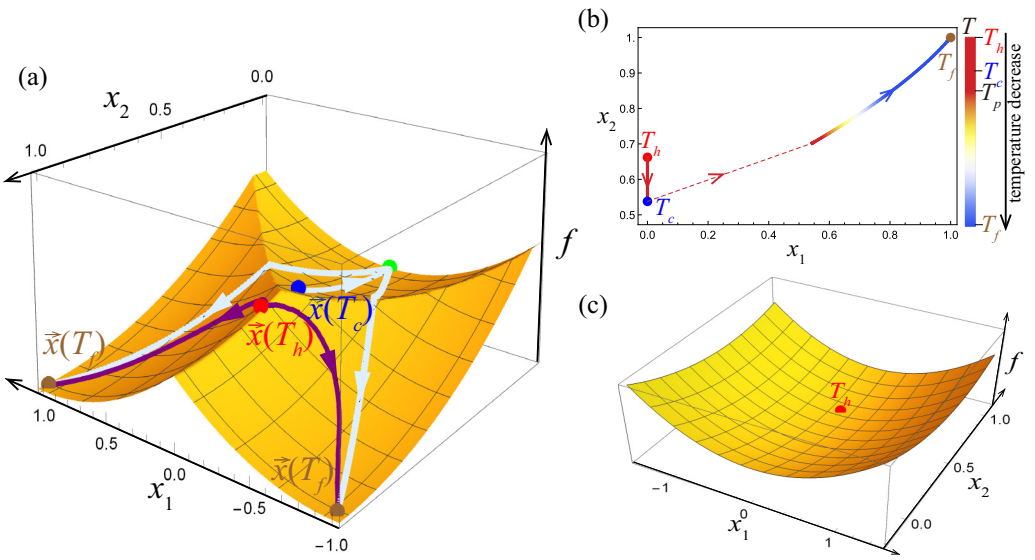

FIG. 1. Schematic diagram of the theoretical model. (a) The surface of free energy at the temperature T_f. (b) The equilibrium line of (x_1, x_2) obtained by Eq. (1) of different temperature. (c) The free-energy surface at the temperature T_h. The red dots correspond to the parameters $\vec{x}(T_h)$ of the equilibrium state of the system with high temperature T_h, and the blue dots correspond to the parameters $\vec{x}(T_c)$ of the equilibrium state of the system with low temperature T_c. The green dot in (a) and brown dots in (a) and (b) represent the metastable state and the equilibrium state of the system with temperature T_f, respectively. The purple lines and white lines with an arrow in (a) represent the nonequilibrium cooling path from the temperature T_h to T_f and T_c to T_f, respectively. The direction of the arrows in (b) is the direction of temperature drop. T_p in (b) is the temperature of the canonical first-order phase transition.

Blume-Emery-Griffiths (BEG) model is given as an example of this theoretical model. Monte Carlo simulations are performed to calculate the phase-transition estimated times for two identical systems, except for different initial temperatures placed at the same low temperature, which demonstrate that the Mpemba effect exists. Their cooling paths validate our theoretical model. The result obtained by us may help to explain the Mpemba effect in water.

The paper is organized as follows. In Sec. II, we introduce the theoretical model and give the reason why the Mpemba effect of the canonical first-order phase transition exists. Then an example of this theoretical model is given in the BEG model in Sec. III. Finally, some conclusions are drawn in Sec. IV.

II. A THEORETICAL MODEL AND ITS ANALYSIS

In this section, we consider a system with two order parameters, x_1 and x_2. In this case, the free energy of the system can be written as $f(T, x_1, x_2)$. From Landau theory, the order parameters corresponding to the equilibrium state is determined by

$$(x_1, x_2) = \arg\min_{(x_1,x_2)} f(T, x_1, x_2). \tag{1}$$

Therefore, for the system with the high initial temperature T_h, the point corresponding to the equilibrium state is at the bottom of the surface of the free energy, as shown in Fig. 1(c), and the order parameters of the points are denoted as $\vec{x}(T_h)(x_{h1}, x_{h2})$. Similarly, the order parameters corresponding to the system with low initial temperature T_c are denoted as $\vec{x}(T_c) = (x_{c1}, x_{c2})$. From Eq. (1), it is easy to get the order parameters of the equilibrium state for the systems with different temperatures. The equilibrium line is plotted in Fig. 1(b). We can see that at the phase-transition point, the equilibrium line is not continuous, indicating that the phase transition is a canonical first-order phase transition.

When the systems with the temperatures T_h and T_c are put into the same cooling environment whose temperature is set to be T_f, the surface of the free energy suddenly changes into a surface with three local minimum points, which is shown in Fig. 1(a). The global minimum points of the free energy are located at $x_1 \neq 0$ and $x_2 \neq 0$ (for example, $|x_1| = 1$ and $x_2 = 1$), which corresponds to the equilibrium state at the temperature T_f. The local minimum points of the free energy are located at $x_1 = 0$ and $x_2 = 0$, corresponding to a metastable state. By marking the point $[x_{h1}, x_{h2}, f(T_f, x_{h1}, x_{h2})]$ which corresponds to $\vec{x}(T_h)$ as well as the point $[x_{c1}, x_{c2}, f(T_f, x_{c1}, x_{c2})]$ which corresponds to $\vec{x}(T_c)$ in Fig. 1(a), it can be seen that $\vec{x}(T_h)$ is closer to the equilibrium state at the temperature T_f than $\vec{x}(T_c)$, while $\vec{x}(T_c)$ is closer to the metastable state. Moreover, we can see that when the nonequilibrium state that corresponds to $\vec{x}(T_h)$ reaches the equilibrium state, it does not need to pass through any free-energy barrier, so it may need only a little time for the phase transition to occur. On the contrary, there is a free-energy barrier between the nonequilibrium state, which corresponds to $\vec{x}(T_c)$, and the equilibrium state, while there is not any free-energy barrier between this nonequilibrium state and the metastable state. Hence, for the system with the low initial temperature, it tends to enter the metastable state first and then it needs quite a long time to pass through a high free-energy barrier from the metastable state to the final equilibrium state. Therefore, for the system with the low initial temperature, it may spend quite a long time cooling to the final equilibrium state. In view of the above two situations, there exists a Mpemba effect.

In a word, the theoretical model of the Mpemba effect through the canonical first-order phase transition we proposed shows that in the cooling processes, the path of the first-order phase transition of the system with the high initial temperature does not pass through any metastable state, while the path of the first-order phase transition of the system with the low initial temperature passes through a metastable state, which leads to the occurrence of the Mpemba effect.

III. AN EXAMPLE OF THE THEORETICAL MODEL

In this section, a specific example of the theoretical model, the Mpemba effect in the BEG model, is proposed to further illustrate our theoretical model.

A. The BEG model and its canonical solution

The BEG model was proposed to study the superfluid transitions as well as the phase separation in He^3-He^4 mixtures [30]. The Hamiltonian of a mean-field BEG model with a nearest-neighbor interaction term can be written as [31–33]

$$H = \Delta \sum_{i=1}^{N} S_i^2 - \frac{J}{2N}\left(\sum_{i=1}^{N} S_i\right)^2 - \frac{K}{2N}\left(\sum_{i=1}^{N} S_i^2\right)^2 + D\sum_{i=1}^{N} S_i S_{i+1}, \tag{2}$$

where J and K are the bilinear exchange interaction parameter and the biquadratic exchange interaction parameter, respectively. Δ is the crystal field of strength parameter, D is the coefficient of the nearest-neighbor interaction, and N is the number of spins. Moreover, S_i is the spin of the ith site of the chain, the value of which can be one of $\{-1, 0, 1\}$. Upon a series of mathematical operations that are shown in Appendix A, the free energy of the system can be expressed by

$$\widetilde{f}(\beta, m, q) = \frac{1}{2}Jm^2 + \frac{1}{2}Kq^2 - \frac{1}{\beta}\ln[\lambda_{\max}(m, q)], \tag{3}$$

where $m = \sum_{i=1}^{N} S_i/N$ is the magnetization per spin, $q = \sum_{i=1}^{N} S_i^2/N$ is the quadrupole moment per spin, $\lambda_{\max}(m, q)$ is the largest eigenvalue of the transfer matrix (see Appendix A for details), and $\beta = (k_B T)^{-1}$ is the inverse temperature. k_B is the Boltzmann constant, which is set to be unity in our calculation. m and q are the order parameters of the system. The free energy per spin of the equilibrium state in the thermodynamic limit ($N \to +\infty$) can be determined by

$$f(\beta) = \min_{m,q} \widetilde{f}(\beta, m, q), \tag{4}$$

and the corresponding parameters m and q are the magnetization and the quadrupole moment per spin of the equilibrium state, respectively. Moreover, we can get the energy per spin of the equilibrium state by

$$\varepsilon(\beta) = f(\beta) + \beta\frac{\partial f(\beta)}{\partial \beta}. \tag{5}$$

B. Canonical first-order phase transition

In the BEG model, $\Delta = 1.07$, $J = 0.5$, $K = 1$, and $D = -0.5$ are set for our discussion. The initial temperature of the high-temperature system is set to be $T_h = 20$ while the initial temperature of the low-temperature system is set to be $T_c = 0.623$, which is just above the transition temperature $T \simeq 0.621$. The temperature of the low-temperature environment is set to be $T_f = 0.05$. The function $\widetilde{f}(\beta, m, q)$ of these three cases is shown in Figs. 2(a), 2(b) and 2(d). When the temperature T of the system is 20, there is only one local minimum point of the function $\widetilde{f}(\beta, m, q)$ with $m = 0$, which is also the global minimum point of the function $\widetilde{f}(\beta, m, q)$. In the case of $T = 0.623$, it is clear to see that there are a total of three local minimum points of the function $\widetilde{f}(\beta, m, q)$, and the minimum value of the local minimum point located at $m = 0$ is smaller than that of the local minimum point located at $m \neq 0$, so the global minimum point of the function $\widetilde{f}(\beta, m, q)$ is still at $m = 0$. As the temperature of the system decreases to $T \simeq 0.621$, the local minimum values of three local minimum points are the same, indicating that they are all global minimum points, which is shown in Fig. 2(c). When the temperature continues to decrease, the global minimum point will no longer be at $m = 0$, which means at $T \simeq 0.621$ the global minimum point jumps from $m = 0$ to $m \neq 0$ and both the equilibrium magnetization per spin m and the equilibrium quadrupole moment per spin q undergo a jump, indicating that it is a canonical first-order phase transition. When $T = T_f = 0.05$, the global minimum points are at about $m = \pm 1$ and $q = 1$.

The energy ε, the quadrupole moment q, and the magnitude of the magnetization $|m|$ per spin of the system in an equilibrium state as a function of temperature T are shown in Figs. 2(e) and 2(f). It can be seen clearly that ε, q, and $|m|$ of the system in an equilibrium state are all discontinuous at the first-order phase-transition point.

C. The time required for the systems with different initial temperature to reach the cryogenic phase

We perform Monte Carlo simulations to see how the magnitude of the magnetization per spin of the system with the high initial temperature $T_i = T_h = 20$ and the system with the low initial temperature $T_i = T_c = 0.623$, which are both put into the same low-temperature environment ($T_f = 0.05$), changes with time. The energy, the magnitude of the magnetization, and the quadrupole moment per spin of the equilibrium state are marked in Figs. 2(e) and 2(f). The detailed Monte Carlo simulation process is shown in Appendix B. The time is defined as the total number of simulation steps divided by the number of spins, or the number of Monte Carlo steps. As shown in Fig. 3(a), we can clearly see that it takes less time for the system with the high initial temperature to reach the cryogenic phase than the system with the low initial temperature, indicating that the Mpemba effect exists. Moreover, we calculate the phase-transition estimated time as a function of the number of spins in the system, which is shown in Figs. 3(b) and 3(c). Here we assume that when the magnetization per spin m and the quadrupole moment per spin q of the system satisfy the relation $(q-1)^2 + (|m|-1)^2 < 0.01$, it enters the cryogenic phase. For the system that has the high

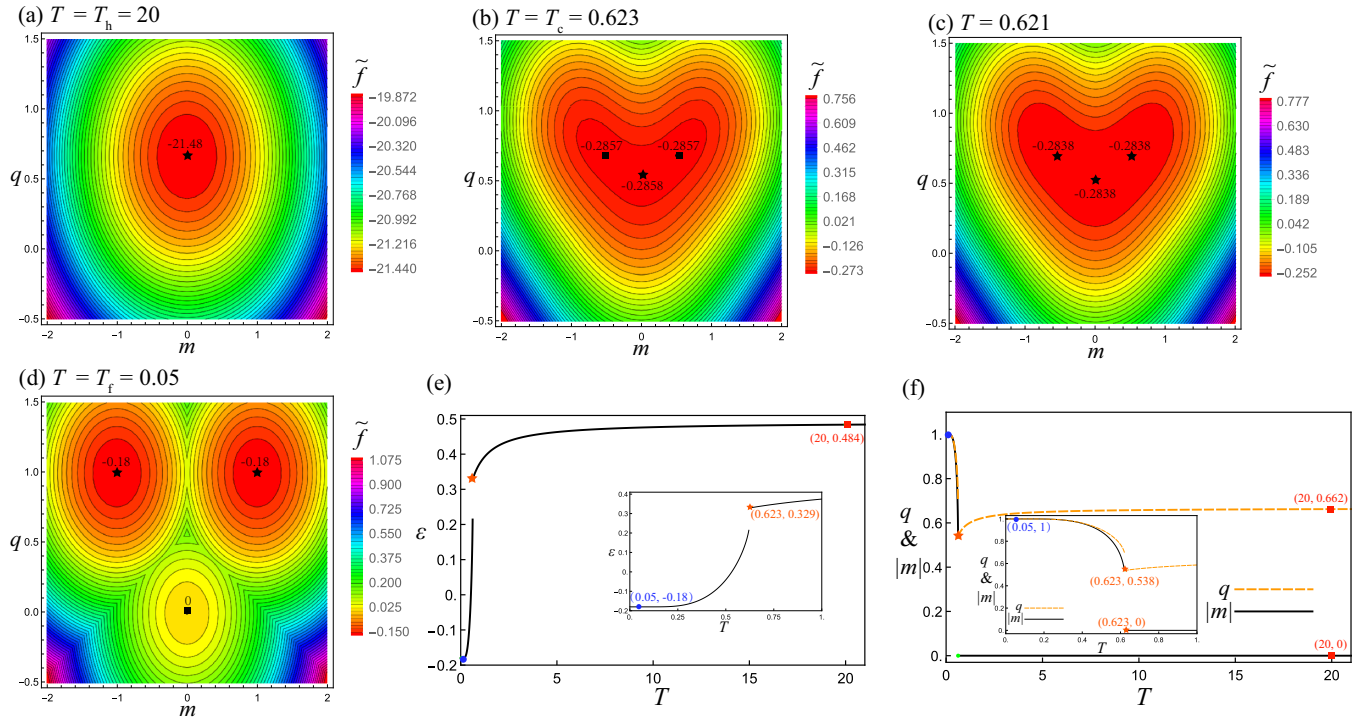

FIG. 2. The free energy per spin $\widetilde{f}(\beta, m, q)$ vs the magnetization per spin m and the quadrupole moment per spin q for four different temperatures T: (a)–(d) the equilibrium energy per spin ε vs the temperature of the system T, (e) the equilibrium quadrupole moment per spin q, and (f) the magnitude of the equilibrium magnetization per spin $|m|$ vs the temperature of the system T. (a) $T = T_h = 20$, corresponding to the system with the high initial temperature. (b) $T = T_c = 0.623$, corresponding to the system with the low initial temperature. (c) $T = 0.621$, which is the temperature of the canonical first-order phase-transition point. (d) $T = T_f = 0.05$, corresponding to the final temperature that the system will reach after cooling down, i.e., the temperature of the environment. The black mark (★) in (a)–(d) represents the global minimum point of $\widetilde{f}(\beta, m, q)$. The black mark (■) in (b)–(d) represents the local minimum point of $\widetilde{f}(\beta, m, q)$. The red mark (■) in (e) and (f) represents the system with the high initial temperature. The orange mark (★) in (e) and (f) represents the system with the low initial temperature. The blue mark (●) represents the final equilibrium state that the system reaches after cooling down.

initial temperature T_h, the phase-transition estimated time τ is approximately proportional to the logarithm of the total number of spins $\lg N$, as shown in Fig. 3(b). On the contrary, the logarithm of the phase-transition estimated time $\lg \tau$ of the system with the low initial temperature T_c is approximately proportional to the number of spins N, which is shown in Fig. 3(c). Therefore, the Mpemba effect of the system is a strong Mpemba effect [35], i.e., it is substantially enhanced on a discrete set of initial temperatures. Contrary to Ref. [35], the strong Mpemba effect mentioned in this paper does not only occur in special initial temperatures, but in a range of temperatures.

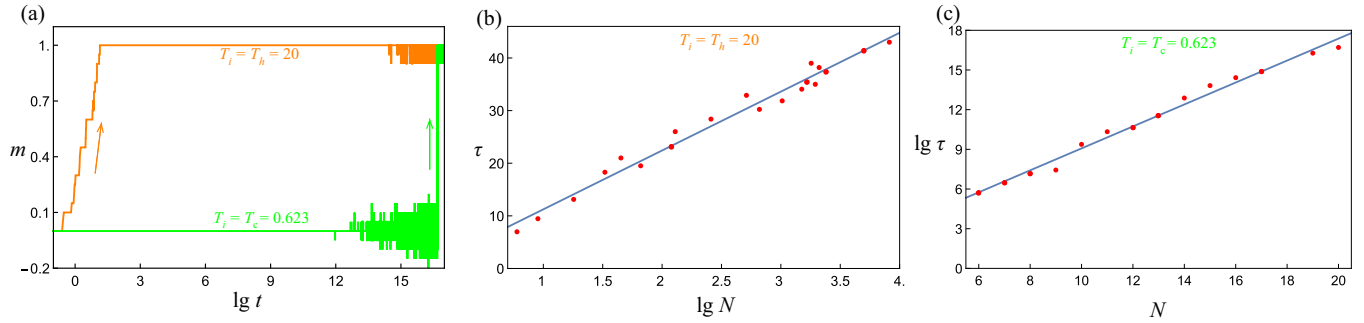

FIG. 3. The magnetization per spin m vs the cooling time of the system t during the cooling process of two systems that have different initial temperature obtained by a Monte Carlo simulation by setting $N = 20$ (a). The canonical first-order phase transition estimated time τ vs the total number of the spin N for two systems which have different initial temperature, (b),(c). The orange line in (a) represents the system with the high initial temperature, while the green line represents the system with low initial temperature. The red dots in (b) and (c) represent the average first-order phase transition estimated time from multiple Monte Carlo simulations, and they are all approximately in a straight blue line, respectively.

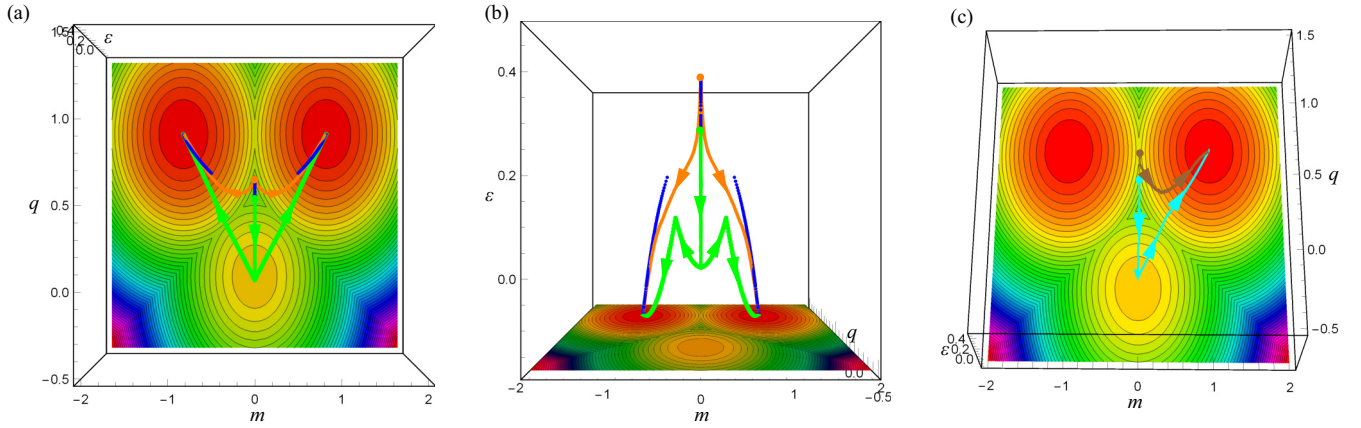

FIG. 4. The average evolution paths taken by the systems of two different initial temperatures during the cooling process, characterized by the energy per spin ε, the magnetization per spin m, and the quadrupole moment per spin q of the system, from two perspectives, (a) and (b). The cooling paths of the systems with two different initial temperatures obtained by a single Monte Carlo simulation, characterized by the energy per spin ε, the magnetization per spin m, and the quadrupole moment per spin q of the system, (c). The dark blue line in (a) and (b) represents the equilibrium energy of the system at different temperatures. The orange line with an arrow in (a) and (b) represents the average cooling path of the system with the high initial temperature $T_i = T_h = 20$. The green line with an arrow in (a) and (b) represents the average cooling path of the system with the low initial temperature $T_i = T_c = 0.623$. The brown line with an arrow and the light blue line with an arrow in (c) represent the cooling paths of the system with the high initial temperature $T_i = T_h = 20$ and the low initial temperature $T_i = T_c = 0.623$, respectively, which are both obtained by a single Monte Carlo simulation.

D. The average evolution paths during the cooling processes

The average evolution paths during the cooling processes for the system with the higher initial temperature and the system with the lower initial temperature, which can be calculated according to the method proposed by Klich *et al.* [35], are shown in Figs. 4(a) and 4(b), and the evolution path obtained by a Monte Carlo single simulation is shown in Fig. 4(c). It is clear that the cooling process of the system does not follow the equilibrium path, thus it is a nonequilibrium process. Moreover, the cooling paths of the system with the higher initial temperature and that with the lower initial temperature are not the same.

For the system with initial temperature $T_i = T_h = 20$, it proceeds directly to the final equilibrium state ($|m| \simeq 1$, $q \simeq 1$) without going through any metastable state. Therefore, the system does not experience any free-energy barriers in this evolution path, leading the phase-transition time τ to reach the final equilibrium state very quickly. Moreover, the phase-transition time τ and the total number of the spins N satisfy the relation $\tau \propto \lg N$ [34].

On the contrary, for the system whose initial temperature is $T_i = T_c = 0.623$, it first enters a metastable state along the paramagnetic path of $m = 0$, and then stays in the metastable state ($m = 0$, $q \simeq 0$) for a long period of time before entering the final equilibrium state ($|m| \simeq 1$, $q \simeq 1$). When the system evolves from the metastable state to the final equilibrium state, it needs to pass through a high free-energy barrier. The system needs to wait for a huge fluctuation to absorb enough energy to overcome the free-energy barrier. Therefore, it takes quite a long time for the system to reach the equilibrium state from the metastable state. Moreover, the time required for the system to reach the metastable state from the initial state is much less than the time required to reach the equilibrium state from the metastable state, indicating that the phase-transition time τ is mainly determined by the latter. In this case, the phase-transition time τ and the total number of spins N satisfy the relation $\lg \tau \propto N$. Comparing the above two situations, we can see that there is a strong Mpemba effect in the system.

The nonequilibrium cooling path and the equilibrium path we obtained is fully in line with the model we propose in Sec. II.

IV. SUMMARY

In summary, we propose a theoretical model of the Mpemba effect through the canonical first-order phase transition. In the process of the canonical first-order phase transition of the system whose initial temperature is high, the system will directly reach the final equilibrium state without being trapped in any metastable state or passing through any free-energy barrier, thus leading to the short phase-transition time. On the contrary, in the process of the canonical first-order phase transition of the system whose initial temperature is low, the system first experiences a metastable state, stays in the metastable state for a long period of time, and then enters the final equilibrium state. And in the process of evolution from the metastable state to the equilibrium state, the system must cross a free-energy barrier, resulting in a long first-order phase-transition time. According to the analysis above, we can see that the Mpemba effect of the theoretical model is actually a strong Mpemba effect.

The BEG model is chosen to further illustrate this theoretical model. The result shows that for the system with the high initial temperature, its first-order phase-transition time τ and the total number of spins N satisfy the relation $\tau \propto \lg N$, while for the system with the low initial temperature, its first-order phase-transition time τ and the total number of spins N satisfy the relation $\lg \tau \propto N$, indicating that the Mpemba effect is

strong. Furthermore, the nonequilibrium cooling path is in line with the expected results of the theoretical model.

From the theoretical model we proposed, it can be seen that the cooling process is a nonequilibrium process while the temperature is a physical quantity of the equilibrium state, so the cooling path of a system is not necessarily its equilibrium path. Going back to the Mpemba effect of water, the evolution paths taken by the freezing of hotter water and colder water may be different. During the cooling process, the water with a high initial temperature does not cool down to the initial state of water with a low initial temperature. Moreover, in the canonical BEG model, there is a metastable state in the cooling path of the system with the low initial temperature, while there is not any metastable state in the cooling path of the system with the high initial temperature, which is the main reason for the strong Mpemba effect. Similarly, there may not be any metastable state in the cooling path of the hotter water, while there may exist a metastable state in the cooling path of the colder water (such as supercooled water [12,13]), leading to the Mpemba effect of the water.

APPENDIX A: THE SOLUTION TO THE CANONICAL PARTITION FUNCTION AND THE FREE-ENERGY FUNCTION OF THE BEG MODEL

The Hamiltonian of the BEG model is

$$H = \Delta \sum_{i=1}^{N} S_i^2 - \frac{J}{2N}\left(\sum_{i=1}^{N} S_i\right)^2 - \frac{K}{2N}\left(\sum_{i=1}^{N} S_i^2\right)^2 + D\sum_{i=1}^{N} S_i S_{i+1}. \tag{A1}$$

The canonical partition function of the system can be written as

$$Z(\beta, N) = \sum_{\{S_i\}} e^{-\beta H} = \sum_{\{S_i\}} e^{-\beta\Delta\sum_{i=1}^{N} S_i^2 + \frac{\beta J}{2N}\left(\sum_{i=1}^{N} S_i\right)^2} \times e^{\frac{\beta K}{2N}\left(\sum_{i=1}^{N} S_i^2\right)^2 - \beta D\sum_{i=1}^{N} S_i S_{i+1}}, \tag{A2}$$

where $\beta = (k_B T)^{-1}$ is the inverse temperature. It can be simplified without squared terms by using the Hubbard-Stratonovich transformation,

$$e^{ab^2} = \sqrt{\frac{a}{\pi}} \int_{-\infty}^{+\infty} e^{-ax^2 + 2abx} dx. \tag{A3}$$

Then Eq. (A2) can be transformed as

$$Z(\beta, N) = \frac{N\beta\sqrt{JK}}{2\pi} \int_{-\infty}^{+\infty}\int_{-\infty}^{+\infty} e^{-\frac{\beta NJ}{2}x^2 - \frac{\beta NK}{2}y^2} \times \sum_{\{S_i\}}\prod_{j=1}^{N} e^{-\beta\widetilde{H}_j} dx\, dy, \tag{A4}$$

where

$$\widetilde{H}_j = \frac{1}{2}\Delta\left(S_j^2 + S_{j+1}^2\right) - \frac{1}{2}Jx(S_j + S_{j+1}) - \frac{1}{2}Ky\left(S_j^2 + S_{j+1}^2\right) + DS_j S_{j+1}. \tag{A5}$$

Using the technique of the transfer matrix, Eq. (A4) can be rewritten as

$$Z(\beta, N) = \frac{N\beta\sqrt{JK}}{2\pi} \int_{-\infty}^{+\infty}\int_{-\infty}^{+\infty} e^{-\frac{\beta NJ}{2}x^2 - \frac{\beta NK}{2}y^2} \times \mathrm{Tr}\{[\mathbf{A}(x, y)]^N\} dx\, dy, \tag{A6}$$

where

$$\mathbf{A}(x, y) = \begin{bmatrix} e^{\beta(Jx+Ky-\Delta-D)} & e^{\frac{1}{2}\beta(Jx+Ky-\Delta)} & e^{\beta(Ky-\Delta+D)} \\ e^{\frac{1}{2}\beta(Jx+Ky-\Delta)} & 1 & e^{\frac{1}{2}\beta(-Jx+Ky-\Delta)} \\ e^{\beta(Ky-\Delta+D)} & e^{\frac{1}{2}\beta(-Jx+Ky-\Delta)} & e^{\beta(-Jx+Ky-\Delta-D)} \end{bmatrix}. \tag{A7}$$

Denoting the largest eigenvalue of the transfer matrix $\mathbf{A}(x, y)$ as $\lambda_{\max}(x, y)$, the canonical partition function of the system can be expressed by

$$Z(\beta, N) = \frac{N\beta\sqrt{JK}}{2\pi} \int_{-\infty}^{+\infty}\int_{-\infty}^{+\infty} e^{-\beta N\widetilde{f}(\beta,x,y)} dx\, dy, \tag{A8}$$

where

$$\widetilde{f}(\beta, x, y) = \frac{1}{2}Jx^2 + \frac{1}{2}Ky^2 - \frac{1}{\beta}\ln[\lambda_{\max}(x, y)] \tag{A9}$$

is the free energy per spin. Actually, it can be proved that $x = \sum_{i=1}^{N} S_i/N = m$ is the magnetization per spin and $y = \sum_{i=1}^{N} S_i^2/N = q$ is the quadrupole moment per spin. We define

$$f(\beta) = \min_{m,q} \widetilde{f}(\beta, m, q), \tag{A10}$$

and we suppose that the global minimum point of $\widetilde{f}(\beta, m, q)$ is located at $m = m_0$ and $q = q_0$. The integral in Eq. (A8) can be evaluated:

$$\begin{aligned}
&\int_{-\infty}^{\infty}\int_{-\infty}^{\infty} e^{-\beta N\widetilde{f}(\beta,m,q)} dm\, dq \\
&= e^{-\beta N f(\beta)} \int_{-\infty}^{\infty}\int_{-\infty}^{\infty} e^{-\beta N[\widetilde{f}(\beta,m,q) - \widetilde{f}(\beta,m_0,q_0)]} dm\, dq \\
&\simeq e^{-\beta N f(\beta)} \int_{-\infty}^{\infty}\int_{-\infty}^{\infty} e^{-\frac{1}{2}\beta N\widetilde{f}_{mm}(m-m_0)^2} \times e^{-\frac{1}{2}\beta N[\widetilde{f}_{qq}(q-q_0)^2 + 2\widetilde{f}_{mq}(m-m_0)(q-q_0)]} dm\, dq \\
&= e^{-\beta N f(\beta)} \int_{-\infty}^{\infty} e^{-\frac{1}{2}\beta N(\widetilde{f}_{mm} - \frac{\widetilde{f}_{mq}^2}{\widetilde{f}_{qq}})(m-m_0)^2} dm \\
&\quad \times \int_{-\infty}^{\infty} e^{-\frac{1}{2}\beta N\widetilde{f}_{qq}[q-q_0 + \frac{\widetilde{f}_{mq}}{\widetilde{f}_{qq}}(m-m_0)]^2} dq \\
&= e^{-\beta N f(\beta)} \sqrt{\frac{2\pi}{N\beta(\widetilde{f}_{mm} - \frac{\widetilde{f}_{mq}^2}{\widetilde{f}_{qq}})}} \sqrt{\frac{2\pi}{N\beta\widetilde{f}_{qq}}} \\
&= \frac{2\pi e^{-N\beta f(\beta)}}{N\beta\sqrt{\widetilde{f}_{mm}\widetilde{f}_{qq} - \widetilde{f}_{mq}^2}},
\end{aligned} \tag{A11}$$

where

$$\widetilde{f}_{mm} = \frac{\partial^2 \widetilde{f}(\beta, m, q)}{\partial m^2}\Big|_{(m,q)=(m_0,q_0)},$$
$$\widetilde{f}_{qq} = \frac{\partial^2 \widetilde{f}(\beta, m, q)}{\partial q^2}\Big|_{(m,q)=(m_0,q_0)}, \tag{A12}$$
$$\widetilde{f}_{mq} = \frac{\partial^2 \widetilde{f}(\beta, m, q)}{\partial m \partial q}\Big|_{(m,q)=(m_0,q_0)}.$$

So the canonical partition function can be evaluated as

$$Z(\beta, N) = \sqrt{\frac{JK}{\widetilde{f}_{mm}\widetilde{f}_{qq} - \widetilde{f}_{mq}^2}}\, e^{-\beta N f(\beta)}. \tag{A13}$$

Therefore, the free energy per spin of the equilibrium state in the thermodynamic limit ($N \to +\infty$) can be obtained by

$$\begin{aligned} f &= -\lim_{N\to+\infty} \frac{\ln Z(\beta, N)}{N\beta} \\ &= \lim_{N\to+\infty} \left[f(\beta) + \frac{1}{N\beta} \ln \sqrt{\frac{JK}{\widetilde{f}_{mm}\widetilde{f}_{qq} - \widetilde{f}_{mq}^2}} \right] \\ &= f(\beta), \end{aligned} \tag{A14}$$

and the corresponding parameters $m = m_0$ and $q = q_0$ are the magnetization and the quadrupole moment per spin of the equilibrium state, respectively.

Moreover, we can get the energy per spin of the equilibrium state by

$$\varepsilon(\beta) = -\frac{1}{N}\frac{\partial \ln Z(\beta, N)}{\partial \beta} = f(\beta) + \beta \frac{\partial f(\beta)}{\partial \beta}. \tag{A15}$$

APPENDIX B: The detailed Monte Carlo simulation process

The Monte Carlo simulation is performed to calculate the estimated time required for the first-order phase transition of the system and the paths of the first-order phase transition in the paper. First, we should obtain the spin configurations corresponding to the system with the high initial temperature and the low initial temperature, respectively. The Monte Carlo simulation method to obtain the spin configuration corresponding to the system of the specific temperature T is as follows:

(i) Randomly generate a spin configuration.

(ii) Randomly choose a spin.

(iii) Randomly generate a random number in $\{-1, 0, 1\}$ and assign it to the spin.

(iv) Calculate the energy change $\Delta E = E_{\text{new}} - E_{\text{old}}$, where E_{new} is the energy of the new spin configuration and E_{old} is the energy of the old spin configuration.

(v) If $\Delta E > 0$, generate a random number (RN) in the interval $[0, 1]$. If $e^{-\Delta E/(k_B T)} \geqslant \text{RN}$, accept the new configuration, otherwise reject the new configuration. If $\Delta E \leqslant 0$, accept the new configuration.

(vi) Repeat steps (ii)–(v) as necessary.

The final spin configuration corresponds to the stable spin configuration at temperature T.

After obtaining the spin configuration corresponding to the system with the high initial temperature and that with the low initial temperature, we perform the Monte Carlo simulation to get the cooling paths of the system as well as the estimated time required for the first-order phase transition to occur. The temperature of the cooling environment is set to $T_{\text{low}} = 0.05$. The Monte Carlo simulation method to obtain the cooling paths and the phase transition estimated time is as follows:

(i) Assign each spin according to the previously obtained spin configuration.

(ii) Calculate the magnetization per spin $m = \sum_{i=1}^{N} S_i/N$, the quadrupole moment per spin $q = \sum_{i=1}^{N} S_i^2/N$, the energy per spin $\varepsilon = H/N$, and the time $t = N_m/N$, where H is the Hamiltonian expressed by Eq. (A1) and N_m is the number of steps for the Monte Carlo simulation that have been performed.

(iii) Calculate $judge = (|m| - 1)^2 + (q - 1)^2$. If $judge < 0.01$, stop the simulation, and the time $\tau = N_M/N$ is the first-order phase-transition estimated time, where N_M is the total steps for the Monte Carlo simulation.

(iv) Randomly choose a spin.

(v) Randomly generate a random number in $\{-1, 0, 1\}$ and assign it to the spin.

(vi) Calculate the energy change $\Delta E = E_{\text{new}} - E_{\text{old}}$, where E_{new} is the energy of the new spin configuration and E_{old} is the energy of the old spin configuration.

(vii) If $\Delta E > 0$, generate a RN in the interval $[0, 1]$. If $e^{-\Delta E/(k_B T_{\text{low}})} \geqslant \text{RN}$, accept the new configuration, otherwise reject the new configuration. If $\Delta E \leqslant 0$, accept the new configuration.

(viii) Repeat steps (ii)–(vii) continuously.

[1] M. Jeng, Am. J. Phys. **74**, 514 (2006).
[2] J. D. Brownridge, Am. J. Phys. **79**, 78 (2011).
[3] E. B. Mpemba and D. G. Osborne, Phys. Educ. **4**, 172 (1969).
[4] J. Jin and W. A. Goddard III, J. Phys. Chem. C **119**, 2622 (2015).
[5] X. Zhang, Y. Huang, Z. Ma, Y. Zhou, J. Zhou, W. Zheng, Q. Jiang, and C. Q. Sun, Phys. Chem. Chem. Phys. **16**, 22995 (2014).
[6] P. Maciejewski, J. Heat Transf. **118**, 65 (1996).
[7] M. Vynnycky and S. Kimura, Int. J. Heat Mass Transf. **80**, 243 (2015).
[8] J. I. Katz, Am. J. Phys. **77**, 27 (2009).
[9] B. Wojciechowski, I. Owczarek, and G. Bednarz, Cryst. Res. Technol. **23**, 843 (1988).
[10] M. Vynnycky and S. L. Mitchell, Heat Mass Transf. **46**, 881 (2010).
[11] G. S. Kell, Am. J. Phys. **37**, 564 (1969).
[12] S. Esposito, R. De Risi, and L. Somma, Physica A **387**, 757 (2008).
[13] D. Auerbach, Am. J. Phys. **63**, 882 (1995).
[14] P. A. Greaney, G. Lani, G. Cicero, and J. C. Grossman, Metall. Mater. Trans. A **42**, 3907 (2011).
[15] A. Lasanta, F. Vega Reyes, A. Prados, and A. Santos, Phys. Rev. Lett. **119**, 148001 (2017).

[16] A. Biswas, V. V. Prasad, and R. Rajesh, Europhys. Lett. **136**, 46001 (2021).
[17] E. Mompó, M. López-Castaño, A. Lasanta, F. Vega Reyes, and A. Torrente, Phys. Fluids **33**, 062005 (2021).
[18] P. Chaddah, S. Dash, K. Kumar, and A. Banerjee, arXiv:1011.3598 (2010).
[19] M. Baity-Jesi, E. Calore, A. Cruz, L. A. Fernandez, J. M. Gil-Narvión, A. Gordillo-Guerrero, D. Iñiguez, A. Lasanta, A. Maiorano, E. Marinari *et al.*, Proc. Natl. Acad. Sci. USA **116**, 15350 (2019).
[20] Y.-H. Ahn, H. Kang, D.-Y. Koh, and H. Lee, Korean J. Chem. Eng. **33**, 1903 (2016).
[21] C. Hu, J. Li, S. Huang, H. Li, C. Luo, J. Chen, S. Jiang, and L. An, Cryst. Growth Des. **18**, 5757 (2018).
[22] N. Vadakkayil and S. K. Das, Phys. Chem. Chem. Phys. **23**, 11186 (2021).
[23] A. Nava and M. Fabrizio, Phys. Rev. B **100**, 125102 (2019).
[24] S. Takada, H. Hayakawa, and A. Santos, Phys. Rev. E **103**, 032901 (2021).
[25] Z. Lu and O. Raz, Proc. Natl. Acad. Sci. USA **114**, 5083 (2017).
[26] Z.-Y. Yang and J.-X. Hou, Phys. Rev. E **101**, 052106 (2020).
[27] Z.-Y. Yang and J.-X. Hou, Phys. Rev. E **105**, 014119 (2022).
[28] C. Luo and J.-U. Sommer, ACS Macro Lett. **5**, 30 (2016).
[29] R. Holtzman and O. Raz, arXiv:2204.03995 (2022).
[30] M. Blume, V. J. Emery, and R. B. Griffiths, Phys. Rev. A **4**, 1071 (1971).
[31] J.-X. Hou, Phys. Rev. E **104**, 024114 (2021).
[32] V.V. Hovhannisyan, N.S. Ananikian, A. Campa, and S. Ruffo, Phys. Rev. E **96**, 062103 (2017).
[33] V.V. Prasad, A. Campa, D. Mukamel, and S. Ruffo, Phys. Rev. E **100**, 052135 (2019).
[34] D. Mukamel, S. Ruffo, and N. Schreiber, Phys. Rev. Lett. **95**, 240604 (2005).
[35] I. Klich, O. Raz, O. Hirschberg, and M. Vucelja, Phys. Rev. X **9**, 021060 (2019).